

# FULL 3D ROI IMAGE RECONSTRUCTION FROM HIGHLY COLLIMATED COMPUTED TOMOGRAPHY

A. Sen<sup>1</sup>, B. G. Bodmann<sup>1</sup>, X. Zhou<sup>2</sup>, K. Li<sup>2</sup>, I. Patrikeev<sup>3</sup>, M. Motamedi<sup>3</sup>, D. Labate<sup>1</sup>, R. Azencott<sup>1</sup>

<sup>1</sup>Department of Mathematics, University of Houston, <sup>2</sup>The Methodist Hospital,  
<sup>3</sup>Health Center for Biomedical Engineering, University of Texas Medical Branch

## ABSTRACT

We introduce a novel method for full 3D Region Of Interest (ROI) reconstruction in computed tomography (CT), called Searchlight CT, which reduces the overall radiation exposure when primarily the reconstruction of a specified ROI is required. To achieve this goal, the Searchlight CT approach restricts the acquisition essentially to X-rays passing through the ROI, yet the algorithm provides a stable and robust reconstruction inside the ROI. The Searchlight CT approach is not limited to a specific mode of acquisition. In fact, it is capable of converting virtually any 3D reconstruction formula into an ROI reconstruction which uses only the radiation which is intersecting the ROI.

## 1. INTRODUCTION AND PREVIOUS WORK

Starting with its introduction in the 1970s, Computed Tomography (CT) has become an essential tool in medical diagnostic and preventive medicine, and its use has increased very rapidly over the last two decades due to technological advances which have made the procedure much more user-friendly. In recent years, the application of CT has expanded even further due to the introduction of new imaging technology including 64-detector scanners for applications such as angiography. However, CT involves exposure of the patient to X-ray radiation with associated health risks essentially proportional to the levels of radiation exposure [1]. Currently an estimated 2% of cancers in the USA may be attributed to the radiation from CT examinations [2].

In order to reduce radiation exposure in CT, several strategies have been explored starting in the 1980's. Most early studies focussed on sparsifying the radiation sources while keeping reconstruction accuracy at a satisfactory level. In fact, since the problem of tomographic reconstruction is ill posed, the general understanding was that incomplete data reconstruction implies some type of approximation of the object to be reconstructed (cf. [3]). Only in 2002 [4], it was shown that one can compute accurate partial 2D reconstructions from incomplete data. Following this result, several methods have been introduced aiming to provide highly accurate or exact ROI reconstruction from partial data including the fan-beam

ROI reconstruction formula in [4] and its variants and extensions (e.g., [5, 6, 7, 8, 9]). Note that these methods are highly specific for a single geometry of acquisition. Furthermore, they impose restrictions on the geometry of the ROI and sometimes require some a-priori knowledge about the object to be reconstructed. Beside this class of analytic methods, several algebraic methods (sometimes called iterative methods) for the reconstruction from incomplete data were also proposed, such as in [10, 11]. The main limitation of algebraic methods is their computational cost, especially for 3D data.

This paper is focussed on the problem of full 3D ROI reconstruction, which has particular relevance in several clinical applications and for which the need to reduce radiation is particularly important. To address this challenge, we propose a novel strategy for 3D ROI reconstruction from incomplete CT data which is not based on specific formulas for specific acquisition modes, nor is an algebraic method. Our algorithmic approach, called Searchlight CT, starts with a black box which can be any analytic formula applicable to CT reconstruction from 3D uncollimated data, and then uses this black box to iteratively reconstruct an ROI using only the projection data of the X-ray passing through the ROI. As a result, our method is 'universal' in the sense that, unlike other ROI reconstruction methods proposed in the literature, it is not restricted to a specific mode of acquisition. In fact, our reconstruction algorithm can be applied to any current CT acquisition method with minor modifications to existing devices. Using only collimated data, our strategy applies the analytic (uncollimated) reconstruction formula associated with the specific mode of acquisition within an iterative algorithmic procedure which includes a specially designed wavelet-based regularization routine to compute an ROI reconstruction. To validate the efficacy and applicability of our approach, the Searchlight CT algorithm was tested for three different modes of acquisitions combined with their respective uncollimated reconstruction formulas: spherical acquisition (with the FBP reconstruction), 3D spiral acquisition (with the Katsevich reconstruction) and circular (C-arm) acquisition (with FDK reconstruction). Our method was tested on both synthetic and experimental data. The results presented in this paper show that the Searchlight CT algorithm provides

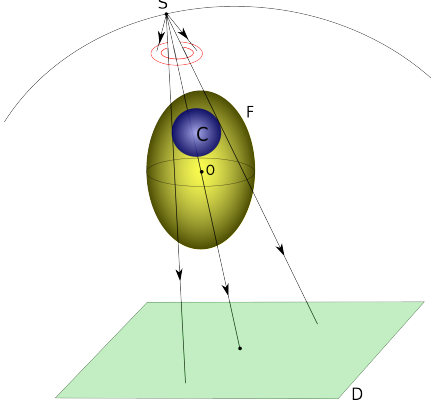


**Fig. 1.** Setup of the Collimated 3D X-ray Tomography

a powerful and general ROI reconstruction method which is a very competitive alternative to the best ROI reconstruction methods recently proposed in the literature.

## 2. COLLIMATED X-RAY TRANSFORM

X-ray Tomography aims to reconstruct the unknown structure of a 3D-object  $F$  by analyzing a set of projection images of  $F$  acquired by measuring radiation attenuation along various straight line paths. For a compactly supported density function  $F$  on  $\mathbb{R}^3$ , the **X-ray Transform** of  $F$  at  $(w, \theta)$  is the line integral of  $F$  over the straight line  $l(w, \theta)$  through the point  $w \in \mathbb{R}^3$  with direction  $\theta \in S^2$ , defined by

$$XF(w, \theta) = \int_{-\infty}^{\infty} F(w + t\theta) dt. \quad (1)$$

In ROI tomography, one is only interested in recovering a region  $C$  included in the support of  $F$ . The **collimation set of rays** will be the set  $T$  of all rays intersecting the region  $C$ , namely

$$T = \{(w, \theta) : l(w, \theta) \cap C \neq \emptyset\}.$$

Our goal is to reconstruct the ROI  $C$  using only the image data associated to the collimation set of rays  $T$  (see Fig. 1). We thus define the **collimated X-ray transform** by

$$\tilde{X}F(w, \theta) = \begin{cases} XF(w, \theta) & (w, \theta) \in T, \\ 0 & (w, \theta) \notin T, \end{cases} \quad (2)$$

In the classical case where the X-ray data are uncollimated, one can recover  $F$  from  $XF$  by the well-known Filtered Back-Projection (FBP) [12] which can be formally expressed as

$$\begin{aligned} F(u) &= X^{-1}(XF)(u) \\ &= \int_{\mathbb{R}^3} \mathcal{F}_2(X_{\theta(\xi)}F)(\xi) e^{i\langle u, \xi \rangle} d\xi, \end{aligned} \quad (3)$$

where  $X_{\theta}F(w) = XF(w, \theta)$ ,  $\mathcal{F}_2$  denotes the 2D Fourier transform on the plane  $h(\theta(\xi))$  orthogonal to the vector  $\theta(\xi)$ , and  $\theta(\xi)$  is any vector orthogonal to  $\xi$ . As is well known [12], a direct application of the Filtered Back-Projection to invert the collimated X-ray transform typically generates multiple undesirable artefacts and is highly inaccurate, particularly for small ROI.

In practice, each arrangement of the source positions around the object determines a specific acquisition geometry. We have selected three classical examples of 3D acquisition geometries, with sources located on a sphere, or on a spiral curve, or on a circle. Note that each of these acquisition geometries is associated with a specific uncollimated reconstruction formula, such as the Katsevich formula for spiral acquisition [13].

### 2.1. Collimated Reconstruction

Due to the ill-posedness of the inversion problem, the standard reconstruction formulas cannot perform acceptable ROI reconstructions using only collimated X-ray data. Our approach can compute accurate ROI reconstructions from collimated data and is applicable to any acquisition geometry for which an uncollimated reconstruction algorithm exists. Our new reconstruction procedure iteratively replaces successive approximations  $f_n$  of  $F$  by updating them inside the ROI  $C$  and regularizing them outside the ROI. The design of the regularization operator, denoted by  $\Lambda$ , is essential for the performance of the algorithm.

Our **Searchlight CT** algorithm, is initialized by setting  $G = \tilde{X}F = 1_T \cdot XF$ , where  $F$  is the unknown density function,  $1_T$  is the indicator function of the collimation set of rays  $T$ , and the dot denotes pointwise multiplication. The initial approximation of  $F$  is given by  $f_0 = X^{-1}G$ , where the operator  $X^{-1}$  denotes any specific uncollimated reconstruction algorithm such as the Katsevich's inversion formula or the FBP procedure. The successive approximations  $f_n$ ,  $n \geq 1$ , of  $F$  are obtained iteratively as follows.

1. Compute the regularized density function  $\Lambda f_n$ .
2. Compute the standard X-ray Transform  $X\Lambda f_n$  of  $\Lambda f_n$ . By splitting the data into the complementary sets  $T$  and  $U = T^c$ , write

$$X\Lambda f_n = 1_T \cdot X\Lambda f_n + 1_U \cdot X\Lambda f_n.$$

3. Replace  $1_T \cdot X\Lambda f_n$  by the known collimated data  $G = 1_T \cdot XF$  in the expression above to obtain  $Y_n = G + 1_U \cdot X\Lambda f_n$ .
4. Compute  $f_{n+1}$  by applying the X-ray uncollimated inversion formula (3) to  $Y_n$  to obtain

$$f_{n+1} = X^{-1}Y_n = Af_n + f_0. \quad (4)$$

where  $A = X^{-1}1_U \cdot X\Lambda$ , and  $f_0 = X^{-1}G$ .

The convergence of this procedure is ensured provided the radius  $r(C)$  of the spherical ROI  $C$  is larger than a critical radius  $\rho$ . For the three acquisition geometries studied here, we have noted that, if  $r(C) > \rho$ , the linear operator  $A$  is a contraction operator in some adequate Banach space, and we conjecture that this will be the case for a large class of X-ray acquisition geometries.

## 2.2. Regularization operator

The objective of the regularization operator is to control the instability induced by the presence of singularities in the data. We found that a highly effective regularization operator is obtained by employing the following wavelet-based method. Specifically, we expand  $F \in L^2(\mathbb{R}^3)$  with respect to a wavelet basis  $\{\psi_{j,k}^\ell\}$ . Note that this expansion produces a representation of  $F$  associated with various scales and locations and that, due to the ability of wavelets to sparsely represent data, the wavelet expansion coefficients of small magnitude are mostly associated with “noise-like” features and can be discarded [14]. Hence we obtain a regularized version of  $F$  by defining a *thresholding regularization operator*. This is essentially a hard thresholding wavelet operator which sets to zero the wavelet coefficients of  $F$  whose magnitude falls below a certain threshold. However, the operator is designed to retain all coarse scale coefficients at scales  $j \leq j_0$ . This allows us to preserve the “global” features of  $F$  and to apply the regularization “locally” outside the ROI  $C$ .

## 3. NUMERICAL EXPERIMENTS

The performance of the Searchlight CT algorithm for collimated reconstruction was validated on 3D Shepp-Logan phantoms and on 3D biological data sets, where collimated acquisition was simulated. Representative 2D slices extracted from the reconstructed three-dimensional ROI are reported in Fig. 2, where our reconstructions are compared with the standard FBP reconstructions. As expected, the direct application of the standard FBP produces unacceptable inaccuracies when applied to collimated data. In these tests, collimated acquisition was simulated assuming that the X-ray emitting source is located at discrete positions on a curve or surface. Data set  $F$  considered had a size of  $257^3$  voxels. The regions of interest  $C$  were chosen to be spherical regions with a radius larger than 40 voxels and arbitrary centers within the sphere of source positions, in general. For the spherical acquisition the source positions lie on a fixed sphere containing the support of  $F$ . For each source position, we simulated collimated acquisition on a planar set of sensors of  $452 \times 370$  pixels. For spiral acquisition, the sources were positioned in a spiral helix of radius 384 voxels and a helical pitch of 35 voxels and 16-row detectors were used. For the regularization operator, Daubechies wavelets Daub4 were used and the thresholding parameter was chosen so that approximately 10% of the

wavelet coefficients were kept.

### 3.1. Performance of the CT Searchlight Algorithm

We quantify performances of the Searchlight CT algorithm by reconstruction accuracy within ROI. For any voxel  $u = (x, y, z)$ , denoting by  $F(u)$  and  $F_{rec}(u)$  the original and reconstructed functions at  $u$ , we define the **Relative Reconstruction Error**  $E_r$  by

$$E_r = \frac{\sum_{u \in C} |F(u) - F_{rec}(u)|}{\sum_{u \in C} F(u)}. \quad (5)$$

The Searchlight CT algorithm takes about 40 iterations to reach an accuracy  $E_r < 0.1$ , provided the radius of  $C$  is sufficiently large. For our data, the radius of  $C$  must be larger than 40 voxels.

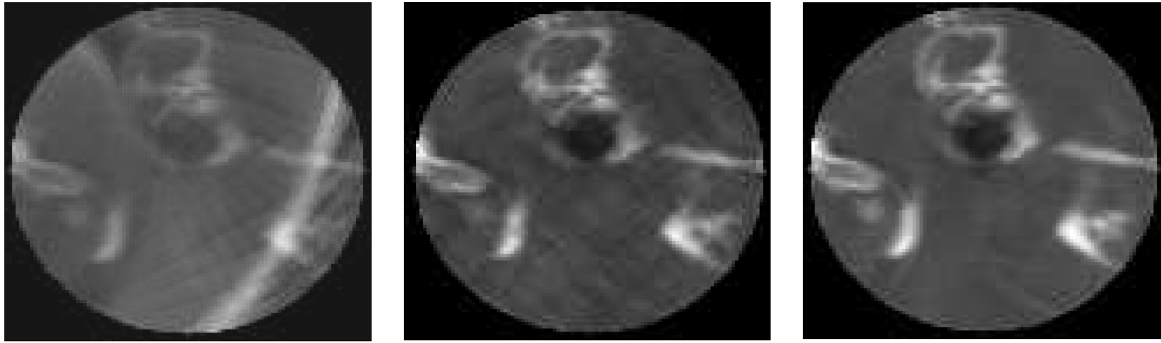
### 3.2. Radiation Exposure

One main motivation for collimated X-ray acquisition is the need to reduce the incident radiation dose. To study radiation dose reduction, we define the radiation dose  $d(u)$  received at a voxel  $u$  as the number of rays passing through  $u$ . Let  $c = \sum_u d(u)$  be the sum of the radiation doses over all voxels in the domain, and call  $m$  be the radiation dose received in the uncollimated case, which is clearly maximal. We then define the **Radiation Exposure**  $R_X$  by  $R_X = \frac{c}{m}$ . As the radius  $r(C)$  of the ROI  $C$  increases, one naturally expects  $R_X$  to increase and the reconstruction error  $E_r$  to decrease. This is confirmed by Table 1, which reports the values of  $R_X$  and  $E_r$ , for several values of  $r(C)$ , in the case of collimated data acquired from the mouse tissue sample using different modes of acquisition (a similar behaviour was found for other data). Note that  $r(C)$  needs to be larger than the critical radius of

**Table 1.** Searchlight CT performances in %

Acquisition mode	Spherical		Spiral		Circular	
	$R_X$	$E_r$	$R_X$	$E_r$	$R_X$	$E_r$
$r(C)$						
45 vox	19	10.8	21	11.4	26	11.3
60 vox	31	8.8	33	9.7	40	9.5
75 vox	44	7.9	47	8.8	55	8.9
90 vox	57	7.5	60	8.4	59	8.6

40 voxels for the algorithm to converge. Our numerical tests also indicate that this convergence holds provided that  $\int_C F$  is larger than  $0.03 \times \int_{\mathbb{R}^3} F$ . We can thus reach exposure reductions up to 75-80% with only a small decrease of reconstruction accuracy. These performances remained stable under data perturbations by white Gaussian noise. Details are not reported here due to space constraints.



(a) Standard Reconstruction

(b) Searchlight CT

(c) Ground Truth

**Fig. 2.** Comparison of reconstruction methods on the mouse tissue data using spiral acquisition. For one typical 2D tissue slice we display three images: (a) Standard Reconstruction, (b) Searchlight CT, (c) Ground Truth

#### 4. CONCLUSION

We have introduced a novel algorithm for ROI reconstruction in full 3D CT which only requires data acquired through highly collimated X-ray focused on a small ROI. This algorithm converges accurately when the radius of the ROI is larger than a critical radius  $\rho$ , independently of the actual data. Our approach provides a promising computational method to preserve accurate image reconstruction in 3D CT while significantly reducing the incident radiation dose through high X-ray collimation. Unlike recently published geometry-specific formulas for ROI reconstruction, our method is not limited to a specific mode of acquisition, but is ‘universal’, yielding a framework which can be easily applied to virtually any existing technology to convert a standard uncollimated reconstruction algorithm into an ROI reconstruction algorithm.

#### 5. REFERENCES

- [1] W. Huda, W. Randazzo, and S. Tipnis et al., “Embryo dose estimates in body ct,” *AJR Am J Roentgenol*, vol. 194, no. 4, pp. 874–880, 2010.
- [2] D. Brenner and E. J. Hall, “Computed tomography. an increasing source of radiation exposure,” *N Engl J Med.*, vol. 357, pp. 2277–2284, 1997.
- [3] R. Clackdoyle and M. Defrise, “Tomographic reconstruction in the 21st century. region-of-interest reconstruction from incomplete data,” *IEEE Signal Processing*, vol. 60, pp. 60–80, 2010.
- [4] F. Noo, M. Defrise, R. Clackdoyle, and H. Kudo, “Image reconstruction from fan-beam projections on less than a short scan,” *Physics in Medicine and Biology*, vol. 47, no. 14, pp. 2525–2546, 2002.
- [5] R. Clackdoyle and F. Noo, “A large class of inversion formulae for the 2-d radon transform of functions of compact support,” *Inverse Problems*, vol. 20, pp. 1281–1291, 2004.
- [6] Y. Ye, H. Yu, and G. Wang, “Exact interior reconstruction with cone-beam ct,” *International Journal of biomedical imaging*, pp. 1–5, 2007.
- [7] M. Defrise, F. Noo, R. Clackdoyle, and H. Kudo, “Truncated hilbert transform and image reconstruction from limited tomographic data,” *Inverse Problems*, vol. 22, no. 3, pp. 1037–1053, 2006.
- [8] G. Zeng and G. Gullberg, “Exact iterative reconstruction for interior problem,” *Physics of Medical Biology*, vol. 54, no. 19, pp. 5805–5814, 2009.
- [9] H. Yu, Y. Ye, S. Zhao, and G. Wang, “Local ROI reconstruction via generalized FBP and BPF algorithms along more flexible curves,” *International Journal of biomedical imaging*, pp. 1–7, 2006.
- [10] G. T. Herman and R. Davidi, “Image reconstruction from a small number of projections,” *Inverse Problems*, vol. 24, no. 4, 2008.
- [11] E. Sidky, C. Kao, and X. Pan, “Accurate image reconstruction from few views and limited angle data in divergent beam CT,” *Medical Physics*, vol. 1, 2009.
- [12] F. Natterer and F. Wubbeling, *Mathematical Methods in Image Reconstruction*. SIAM: Society for Industrial and Applied Mathematics, 2001.
- [13] A. Katsevich, “Theoretically exact fbp-type inversion algorithm for spiral ct,” *SIAM Journal of Applied Mathematics*, vol. 62, no. 6, pp. 2012–2026, 2002.
- [14] S. Mallat, *A Wavelet Tour of Signal Processing*, 3rd ed. Academic Press, 2008.